Urban Forestry & Urban Greening 81 (2023) 127866

Contents lists available at ScienceDirect

Urban Forestry & Urban Greening

journal homepage: www.elsevier.com/locate/ufug

Object-based classification of urban plant species from very high-resolution satellite imagery

Pierre Sicard[a,*], Fatimatou Coulibaly[a], Morgane Lameiro[b], Valda Araminiene[c], Alessandra De Marco[d], Beatrice Sorrentino[d], Alessandro Anav[d], Jacopo Manzini[e], Yasutomo Hoshika[e,f], Barbara Baesso Moura[e], Elena Paoletti[e,f]

[a] ARGANS Ltd, Sophia Antipolis, France
[b] Ville de Aix-en-Provence, Direction des Espaces Verts, Aix-en-Provence, France
[c] LAMMC, Girionys, Lithuania
[d] ENEA, Rome, Italy
[e] IRET-CNR, Sesto Fiorentino, Italy
[f] National Biodiversity Future Center, Palermo, Italy

ARTICLE INFO

Keywords:
Urban Forest
Urban Green Infrastructure
VHR
Spectral feature
Textural feature
Classification
WorldView-2

ABSTRACT

Cities are facing too many challenges. Urban vegetation, in particular trees, are essential as they provide services in terms of air pollution mitigation, freshness, biodiversity, and citizens' well-being. Accurate data on location, species, and structural characteristics are essential for quantifying their benefits. However, the cost of measuring thousands of individual trees through field campaigns can be prohibitive and reliable information on domestic gardens is lacking due to difficulties in acquiring systematic data. The main objective of this study was to investigate the suitability of very-high resolution satellite imagery, e.g., WorldView-2, for detecting, delineating, and classifying the urban plant species in both public and private areas. The characterization of urban vegetation is difficult due to the complexity of the urban environment (buildings, shadows, open courtyards), the diversity of species and the spatial proximity between trees. To overcome these constraints, an object-based classification was developed with the selection of new relevant spectral and texture-based features for each plant species. Four spectral bands (blue, green, yellow, red) and four texture features (i.e., energy, entropy, inverse difference moment, Haralick correlation) were found to be the most efficient attributes for object-based classification from WV-2 images. Then, a classification of plant species, by using a Random Forest classifier, and ground validation were performed. In the two study areas, Aix-en-Provence (France) and Florence (Italy), 22 and 20 dominant plant species, and grassland, were identified and classified with an overall accuracy of 84% and 83%, respectively. The highest classification accuracy was obtained for *Pinus* spp. and *Platanus acerifolia* in Aix-en-Provence, and for *Celtis australis* and *Cupressus sempervirens* in Florence. The lowest classification accuracy was obtained for *Quercus* spp. in Aix-en-Provence, and *Magnolia grandiflora* in Florence.

1. Introduction

Global warming and air pollution are two major concerns affecting biodiversity, life quality, citizens well-being and human health (Anenberg et al., 2022; Malashock et al., 2022; Southerland et al., 2022; Sicard et al., 2023), in particular in cities where 56% of the world population lived in 2020 (United Nations, 2020). Following successive heatwaves and the COVID-19 pandemic, the European cities with more than 20,000 inhabitants have to establish "*ambitious Urban Greening Plans*" by including nature-based solutions and greening strategies by 2030 (European Union Biodiversity Strategy for 2030, COM (2020)380 final) to both mitigate the effects of air pollution and climate change and adapt to them. Urban trees are the most important elements of urban ecosystems (Ostberg et al., 2018), and contribute to reduce air pollution in cities (Baró et al., 2015; Salbitano et al., 2016; Nowak et al., 2018; Sicard et al., 2018; Pace et al., 2021), increase carbon stock (Proietti et al., 2016), mitigate the urban heat islands (Manes et al., 2012; Ren et al., 2022), provide cooling and shading (Rahman et al., 2020), regulate

* Corresponding author.
E-mail address: psicard@argans.eu (P. Sicard).

https://doi.org/10.1016/j.ufug.2023.127866
Received 15 October 2022; Received in revised form 14 December 2022; Accepted 6 February 2023
Available online 9 February 2023
1618-8667/

water runoff (Pataki et al., 2011), reduce noise (Klingberg et al., 2017) as well as provide social and psychological benefits, enhancing citizens' well-being and human health (Samson et al., 2019; Ugolini et al., 2020).

Information about the individual tree, accurate data on location, species, and structural characteristic such as tree height and crown diameter are essential to quantify the environmental and social benefits of urban trees (e.g., Manes et al., 2016; Russo et al., 2016; Fusaro et al., 2017; Pace et al., 2018; Pu and Landry, 2019). Most of these data are derived from municipal tree inventories (e.g., Selmi et al., 2016), which include only public trees managed by the municipality representing e.g., about 36% of full stocking in 50 cities in the United States (McPherson et al., 2016). Tree inventories can also be obtained from field visits by visual observations (Nowak et al., 2013; Persson, 2016). This method is often expensive and time-consuming (Klingberg et al., 2017), and inefficient at larger scales when the tree species distribution is heterogeneous (Nowak et al., 2008; Westfall, 2015; Persson, 2016), making remote sensing more attractive (Klingberg et al., 2017).

Shojanoori and Shafri (2016) performed an extensive literature review on the use of remote sensing for forestry applications, particularly for tree species detection. During the last decades, the use of aerial photography and airborne laser scanning, such as LiDAR data, was widely used and considered as the most accurate remote sensing technique to estimate forest attributes (e.g., Singh et al., 2015; Alonzo et al., 2016; Persson, 2016; Song et al., 2016; Chen et al., 2017; Solano et al., 2019). The high cost coupled with the spatial, temporal, and spectral resolution of such techniques are the main limiting factors to using LiDAR to investigate individual trees (Key et al., 2001; Shojanoori and Shafri, 2016). In most of the previous studies, tree attributes were derived from satellite imagery at moderate spatial resolution such as Landsat (Manes et al., 2012; Silli et al., 2015; Marando et al., 2016) and sensors like Moderate Resolution Imaging Spectro-radiometer (Manes et al., 2016; Bottalico et al., 2017). Remote sensing, with high spatial and spectral resolution, and Geographical Information Systems (GIS) could be cost-effective and consistent techniques to get information about individual trees (Larondelle et al., 2014; Alonzo et al., 2016; Parmehr et al., 2016; Fusaro et al. 2017), when employed with useful tools in Mapping and Assessment of Ecosystem Services (Maes et al., 2016).

Since 2000, the spatial resolution of the optical very high resolution (VHR) satellite sensors allows detecting and estimating some tree attributes at landscape scale (Table 1S), e.g., Geoeye-1 (Qian et al., 2020), IKONOS (Pu and Landry, 2012), WorldView (Immitzer et al., 2012; Pope and Treitz, 2013; Nouri et al., 2014; Li et al., 2015; Pu et al., 2015; Choudhury et al., 2019; Kokubu et al., 2020), and Pléiades (Beguet et al., 2014; Lefebvre et al., 2016; Akbari and Kalbi, 2016; Effiom, 2018; Pu and Landry, 2019) at a lower cost compared to field observations or airborne laser scanning (Persson, 2016). Compared to IKONOS, the WV-2 sensor has a greater capability to classify tree species (Pu and Landry, 2012), and the Pléiades and WV-2 images perform equally well for estimation of forest attributes (Persson, 2016). Such steerable optical sensors allow fast and frequent stereo or tri-stereo acquisitions of cloud-free images over larger areas within a short interval of time (Persson, 2016).

Most of the previous studies, using very high spatial resolution satellite imagery, were limited to rural and forested areas (e.g., Immitzer et al., 2012; Pu and Cheng, 2015; Akbari and Kalbi, 2016; Modica et al., 2016; Solano et al., 2019). The detection of individual trees and species differentiation are challenging in cities, as trees can be isolated, lined up or grouped in patch, with a wide range of plant species, high spectral similarity of vegetation types, and high-density stands, trees in the shade, trees with low spectral contrast, and proximity of neighboring buildings (Alonzo et al., 2015; Parmehr et al., 2016; Klingberg et al., 2017; Choudhury et al., 2019). In addition, private gardens are an important component of urban landscape and urban green infrastructure, for instance contributing to 35-47% of the total urban green spaces in the United Kingdom (Loram et al., 2007). The potential contribution of residential areas and yards to overall urban sustainability is recognized worldwide (Owen, 2010; Cameron et al., 2012; Vila-Ruiz et al., 2014; Zhang and Jim, 2014), and could make significant contributions to urban biodiversity and ecological richness in cities (Smith et al., 2006; Müller et al., 2010; Cameron et al., 2012). However, their relative value within the wider urban green space is difficult to quantify and hence their measurable benefits is rarely assessed (Cameron et al., 2012; Zhang and Jim, 2014).

For a realistic and proper quantification of the benefits of urban vegetation in terms of providing ecosystem services such as mitigation of air pollution and urban heat island, and above-ground carbon storage at city scale, a consistent inventory of vegetation within private and public areas, is needed to avoid a large underestimation and to establish an efficient Urban Greening Plan and carbon footprint (Sicard et al., 2018; Pretzsch et al., 2021). As tree species diversity is a major factor in providing ecosystem services in cities (Grote et al., 2016; Galle et al., 2021), the large variety of tree species cannot be classified as a single vegetation category (e.g., conifers, broadleaves, and mixed species) as previously performed in studies (e.g., Manes et al., 2016; Bottalico et al., 2017).

For individual tree classification in urban areas, previous studies have reported that the classification algorithm produced better results by using object-based (overall accuracy: 77%) than pixel-based approach (overall accuracy: 73%) due to high spectral variability (Pu et al., 2011). By using pixel-based classification, the spectral response of individual trees can be influenced by canopy exposition (sunlit/shaded) and shaded canopy due to nearby buildings, reducing the overall accuracy (Quackenbush et al., 2000). The object-based image analysis includes spectral, textural, and spatial features, suitable for individual tree species classification in urban environments (Zhang and Qiu, 2012; Zhou, 2013; Puissant et al., 2014; Lefebvre et al., 2016; Shojanoori and Shafri, 2016; Choudhury et al., 2020). In literature, the object-based classification was performed using two machine learning approaches: Random Forest (e.g., Puissant et al., 2014; Boukir et al., 2015; Immitzer et al., 2016; Lefebvre et al., 2016; Huesca et al., 2019) and Support Vector Machine (e.g., Adam et al., 2014; Deur et al., 2020). The Random Forest classifier showed a performance of 89% to classify different textures with the co-occurrence matrix (Boukir et al., 2015).

Several studies used VHR images for some tree species identification in urbanized areas (Pu et al., 2011; Pu and Landry, 2012; Li et al., 2015; Choudhury et al., 2020), but none focused on identifying vegetation in both private and public lands. The structural diversity of the vegetation in residential yards can be a good predictor of biological diversity in the urban environment (Müller et al. 2010). However, identifying plant species in private areas is challenging due to i) spatial complexity in courtyards with building and shadows presence, and ii) high plant species diversity compared with trees in the public space such as street trees. Previous studies have reported 60-70% of non-native species in

Table 1
WorldView-2 imagery properties related to the acquisition over the study areas.

Study area	Date	Off-nadir angle (°)	Viewing angle (°)		Sun elevation angle (°)	Sun azimuth angle (°)	Sat azimuth angle (°)
			Across	Along			
Aix	17/07/2020	23.90	15.80	18.30	62.10	136.60	179.82
Florence	30/07/2020	18.20	-17.9	-3.30	35.70	158.90	201.9

private residential gardens in temperate cities (e.g., Smith et al. 2006; Cilliers et al. 2012; Vila-Ruiz et al., 2014).

Trees at public roadside and green spaces have been studied, but those in private properties were largely ignored (Cameron et al., 2012; Zhang and Jim, 2014). Reliable information on domestic gardens is lacking, mainly due to difficulties in acquiring systematic data (Cameron et al., 2012, Zhang and Jim, 2014). Therefore, studying the vegetation characteristics within private areas has become a research priority in cities (Vila-Ruiz et al., 2014; Zhang and Jim, 2014). The aim of this study was to assess the potential of VHR satellite images for classifying plant species and mapping geo-located urban vegetation and greenspaces in both public and private land over two study areas in two cities, Aix-en-Provence (France) and Florence (Italy). We developed a object-based classification using the spectral and textural characteristics and image segmentation for detection, delineation, and classification of urban tree canopies and herbaceous areas. To our best knowledge, this is the first work using VHR satellite images for detecting, extracting, and classifying more than 20 individual dominant plant species, among hundreds of thousands tree canopies detected in both private and public areas, over large urban areas (50-80 km^2) at high classification accuracy.

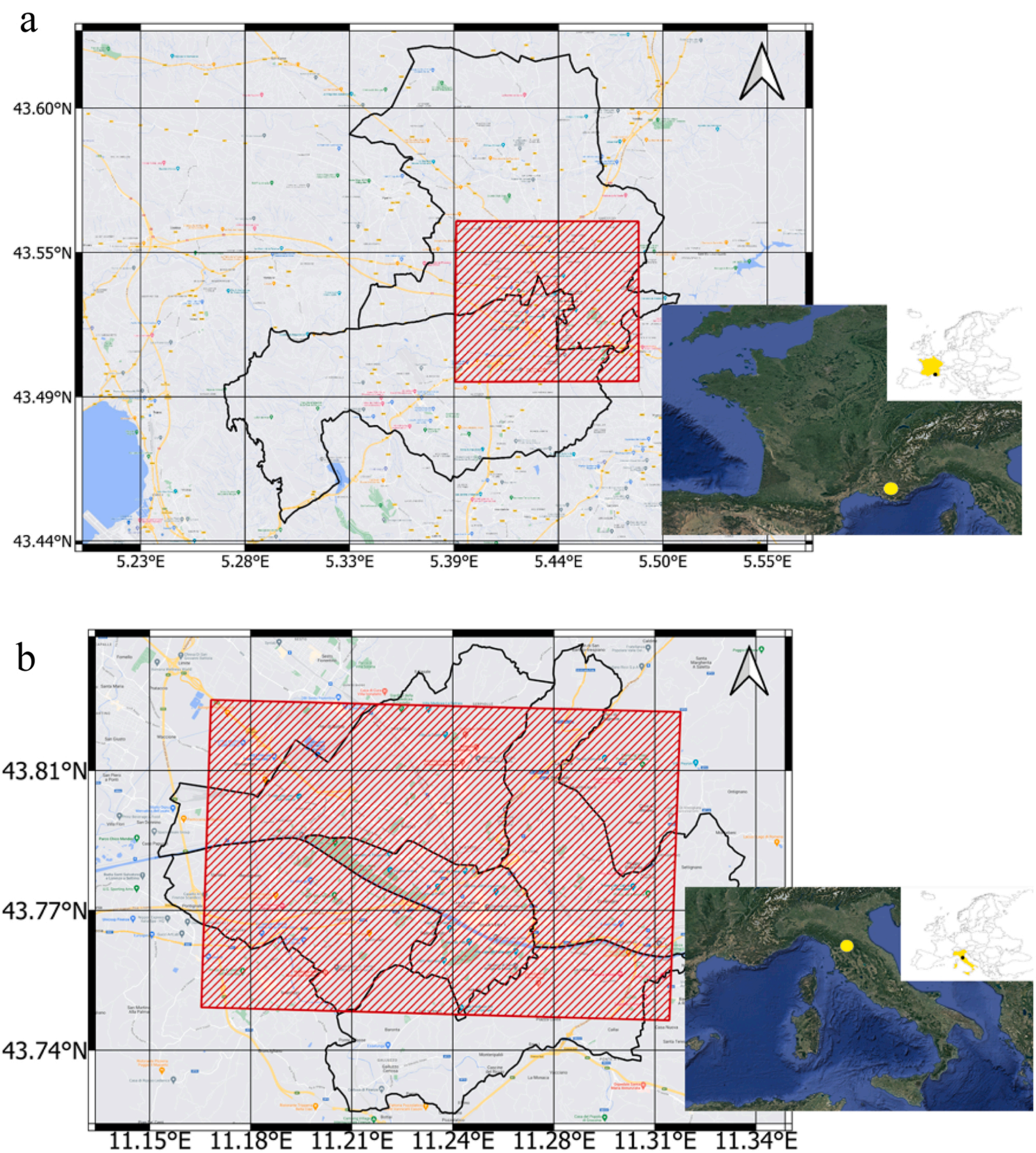

Fig. 1. Location of both front runner cities: a) Aix-en-Provence (France) and b) Florence (Italy). The study area, covered by the satellite image (slashed red areas), extends over 50 km^2 in Aix-en-Provence and 80 km^2 in Florence.

2. Materials and methods

2.1. Study areas

2.1.1. Aix-en-Provence, France

Southern France is characterized by strong urbanization pressures and increasing vulnerability to climate change (Sicard and Dalstein-Richier, 2015). The population of Aix-en-Provence, located near Marseille, is estimated at approximately 143,000 people over a total surface area of 186 km^2. The municipality Aix-en-Provence has a Mediterranean climate (Köppen-Geiger classification). The mean annual precipitation and temperature are 568 mm and 13.6 °C, respectively.

2.1.2. Florence, Italy

The municipality of Florence, capital of the Tuscany region located in central Italy (Fig. 1), accounts for approximately 380,000 inhabitants, and is characterized by a hot-summer Mediterranean climate (Köppen-Geiger classification). The mean annual precipitation and temperature are 845 mm and 15.2 °C, respectively.

2.2. Public tree inventory

Both cities have an exhaustive public trees inventory (e.g., location, species, and age) which are maintained by the municipalities who are responsible for watering, pruning, and monitoring tree health in general. The municipality of Aix-en-Provence established a Tree Charter in November 2017, i.e., a master plan to protect and develop its public tree heritage, and to raise public awareness of the benefits provided by urban trees. Both independent public tree inventories were mapped using QGIS (Fig. 2) and used in this study as training samples (70% of the inventory data) and as validation dataset (30% of the inventory data).

In 2019, the municipality of Aix-en-Provence accounts for 180 ha of green spaces including about 31,000 inventoried public trees managed by the municipality (Fig. 2a). The ten most abundant tree species, representing about 75% of all inventoried public trees (Table 2S), are *Celtis australis* (13.8%), *Platanus acerifolia* (12.3%), *Pinus* spp. (11.9%), *Cupressus sempervirens* (9.2%), *Acer* spp. (6.5%), *Tilia* spp. (4.9%), *Sophora japonica* (4.4%), *Populus* spp. (3.2%), *Cercis siliquastrum* (3.1%) and *Fraxinus angustifolia* (2.8%). In the historical city center and on the fringe, most trees grow along boulevards, squares (*Platanus acerifolia, Celtis australis*), and private gardens. Seven public urban parks, extending over 65 ha, accounts for 3,500 trees with more than 50 tree species e.g., *Pinus* spp., *Cedrus libani*, *Cupressus sempervirens, Tilia* spp., and *Cercis siliquastrum*.

In 2019, the municipality of Florence accounts for 236 ha of green spaces including about 75,700 inventoried public trees managed by the municipality (Fig. 2b) with 115 different tree species growing in streets, urban parks, and peri-urban forests (Pauleit et al., 2005). In the city center, most trees grow in private gardens and public squares. The ten most abundant tree species, representing about 65% of all inventoried public trees (Table 2S), are *Tilia x europaea* (10.9%), *Cupressus sempervirens* (9.7%), *Celtis australis* (8.9%), *Quercus ilex* (8.5%), *Pinus pinea* (5.8%), *Platanus x acerifolia* (5.7%), *Olea europaea* (4.7%), *Ulmus* spp. (4.3%), *Acer campestre* (2.6%) and *Robinia pseudoacacia* (2.3%).

2.3. Satellite-based approach

The flowchart of the procedure is shown in Fig. 3. Python, Geospatial Data Abstraction Library (GDAL), Orfeo Toolbox (OTB) and Quantum Geographic Information System (QGIS) were used in the post-processing of segmentation, classification, and mapping of results.

2.3.1. Satellite image sets

Among all VHR satellites and images (Table 1S), we have selected the images available over both municipalities (Fig. 1) in summer 2020 for ground validation, cloud free sky condition ($<$ 2% of the image covered by clouds), and with low view angle to limit the displacement of images. Based on all criteria, we selected the WV-2 images (DigitalGlobe, USA) acquired on 17 July 2020 in Aix-en-Provence and on 30 July 2020 in Florence (Fig. 1S) with an off-nadir view angle of 23.90° and 18.20°, respectively (Table 1). The WV-2 includes one panchromatic band (PAN, 450-800 nm) of 0.5 m spatial resolution and eight multispectral (MS) bands of 2 m resolution: coastal, 401-450; blue, 450-510 nm; green, 510-580 nm; yellow, 588-627 nm; red, 630-690 nm; red-edge, 703-743 nm; near-infrared-1, 770-890 nm; and near-infrared-2, 861-954 nm. The images were delivered as orthorectified processing level, including corrections for radiometric and sensor distortions. The image had a 16-bit radiometric resolution. The images cover a 50-km^2 study area over Aix-en-Provence, centered on urbanized part of the municipality, and an 80-km^2 study area over Florence, i.e., 78% of the entire municipality (Fig. 1).

2.3.2. Image preprocessing

First, an atmospheric correction was conducted for each satellite image, in which the top-of-atmosphere radiance received by sensors was converted to ground surface reflectance, to enhance spectral differentiation among multiple surface components (Pu et al., 2015; Deur et al., 2020). Both WV-2 images were calibrated by using the parameters (e.g., ozone, and water vapor absorption) provided by the imagery auxiliary metadata (Kizel et al., 2017). We used the Dark Object Subtraction technique for atmospheric scattering correction of MS data (Chavez, 1988).

Next, the MS orthorectified and radiometrically corrected images were fused with corresponding PAN images by using a pan-sharpening method. The pan-sharpening of lower resolution MS and higher resolution PAN images is important for object detection, segmentation, and classification (Jones et al., 2020) to improve the accuracy of photo-analysis and feature extraction (Sarp, 2014). This pan-sharpening approach was already used in cities (e.g., Nichol and Wong, 2007). The high-performance pan-sharpening algorithms used in remote sensing are the Brovey, Gram-Schmidt, and Principal Component Analysis techniques (Sarp, 2014). The “weighted” Brovey algorithm was adopted in this analysis using the processing script of the GDAL. In the Brovey sharpening process, a pseudo-PAN intensity is computed, and each MS pixel is multiplied by the ratio of the PAN pixel intensity over the pseudo-PAN intensity (Bovolo et al., 2010; Sarp, 2014).

$$\mathrm{DN}_{\mathrm{fusedMSi}} = \frac{\mathrm{DN}_{\mathrm{bi}}}{\mathrm{DN}_{\mathrm{b1}} + \mathrm{DN}_{\mathrm{b2}} + \ldots + \mathrm{DN}_{\mathrm{bn}}}\mathrm{DN}_{\mathrm{PAN}}$$

where *DN* is the digital number of that band and *bi* is the band of the MS image. The pan-sharpening processing resulted in WV-2 images of 0.5 m of spatial resolution across the full eight spectral bands (Fig. 2S) by fusing the 2 m MS image with the 0.5 m PAN image.

2.3.3. Stepwise masking system

A stepwise masking system was performed at two levels, with thresholding and morphological operations (Fig. 3), to increase the relative spectral separability and improve the accuracy of plant species mapping (Pu et al., 2008; Pu, 2011). After radiometric calibration and pan-sharpening of WV-2 data, both study sites were separated into vegetated and non-vegetated areas by using a pixel-based approach with a Normalized Difference Vegetation Index (NDVI) threshold (Lefebvre et al., 2016).

$$\mathrm{NDVI} = \frac{\rho_{\mathrm{NIR}} - \rho_{\mathrm{red}}}{\rho_{\mathrm{NIR}} + \rho_{\mathrm{red}}}$$

where ρ_{NIR1} and ρ_{red} are spectral reflectance measurements acquired in the near-infrared-1 and red (visible), respectively.

The optimal NDVI threshold was first defined from the NDVI histogram and by image interpretation, and then by refining it at a ±0.01 step interval to determine the optimum threshold matching when compared

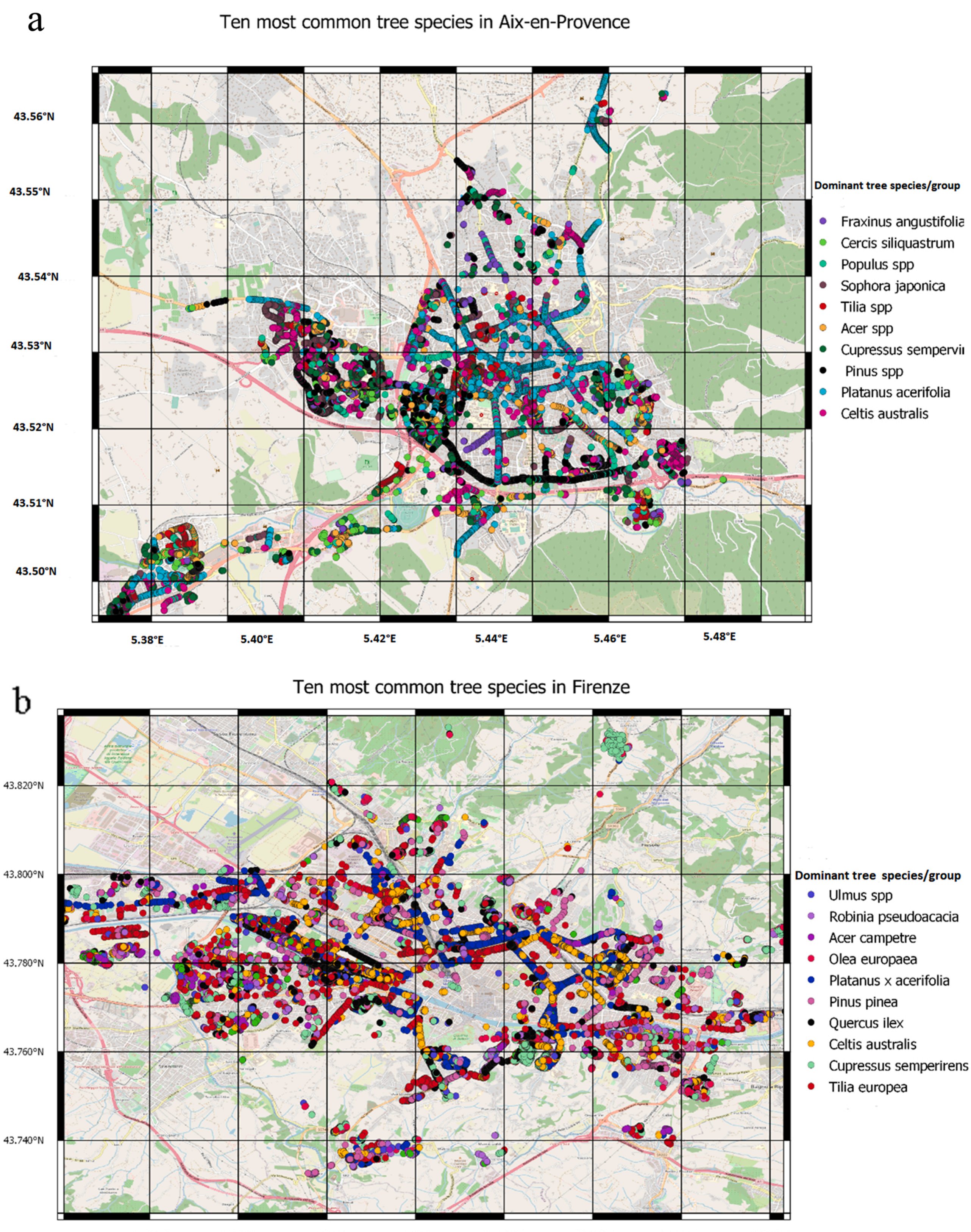

Fig. 2. Public trees inventory (e.g., location, species) which are under the municipalities' responsibility with the ten most common tree species in Aix-en-Provence (a) and Florence (b).

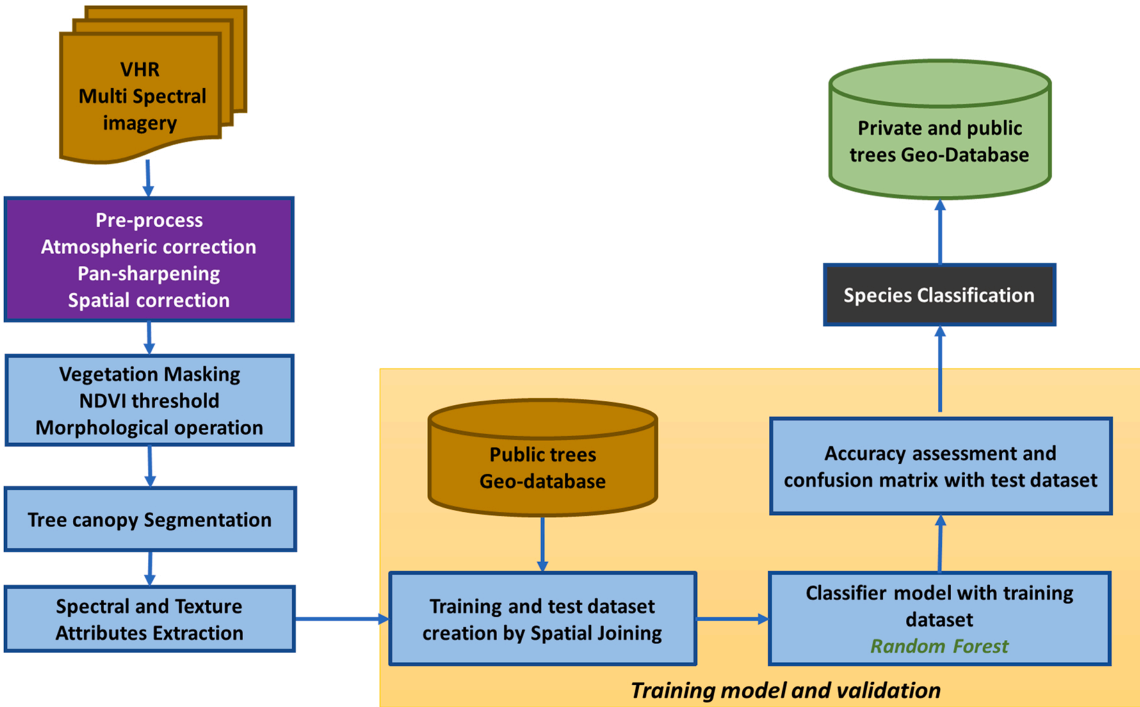

Fig. 3. Flowchart of the analysis procedure of identifying, delineating, and classifying urban plant species/groups with high resolution WV-2 imagery.

to reference data (Pu and Landry, 2012). For the classification, the pixels with an NDVI above 0.40 and 0.55 were classified as vegetated areas in Aix-en-Provence and Florence, respectively, while the pixels with a lower NDVI were classified as non-vegetated areas (i.e., buildings, sidewalks). Individual trees, isolated, lined-up or grouped, can be easily detected (Fig. 3S). A morphological operation (named "erosion") on the vegetation mask, with a ball structuring element having three-pixel radius, was performed to remove shadows around trees.

2.3.4. *Image segmentation*

An image segmentation into polygons (or objects) representing the vegetated areas (i.e., group of pixels spatially adjacent and spectrally similar) was performed to contour individual trees, urban forests, shrubs, and grasses (lawn/turf). The watershed algorithm was used for different window sizes (from 5 to 20 pixels) and different ranges of DN (from 100 to 250 DN). Small window size (e.g., 5 pixels) and small range of DN (e.g., 100) led to over-segmentation effects (Niccolai et al., 2010). One the other side, using large window size and range of DN led to under-segmentation effects (Fig. 4). The watershed algorithm was finally used with a window size of 10 pixels and a range of 150 DN (Fig. 4). Reproducing this kind of delineation by using an automated segmentation algorithm is challenging but essential for an operational large-scale application of the method. The crown delineation by watershed segmentation is ideally suited for classification (Blaschke, 2010; Niccolai et al., 2010). Finally, spectral, and spatial features are computed for each object to characterize textural properties of each vegetated area, i.e., tree crown and grass bed (Pu and Cheng, 2015).

2.3.5. *Texture-based features extraction*

Statistical textural analysis can be used to consider the inter-spatial relations of spectral values within pixels (Maack et al., 2015). The co-occurrence analysis, in particular the Grey Level Co-occurence Matrix (GLCM) method with related attributes, is widely used in remote sensing studies (e.g., Regniers, 2014; Beguet et al., 2014; Maack et al., 2015; Immitzer et al., 2016; Lefebvre et al., 2016). In this study, ten Haralick texture-based attributes (Table 3S) were calculated from a GLCM for each spectral band while keeping only vegetated areas. The selected texture-based features have demonstrated their potential in estimating plant traits with VHR satellite images (e.g., Regniers, 2014; Beguet et al., 2014; Lefebvre et al., 2016; Zhou et al., 2017).

For texture feature extraction, we used the eight spectral bands, however the attributes from four visible bands (blue, green, yellow, and red) visually showed a texture within canopy, highlighting that they are relevant to describe it (Fig. 5). A principal component analysis was applied to extract the most useful texture-based attributes from both WV-2 images (Knauer et al., 2019; Deur et al., 2020). Four Haralick texture attributes (i.e., energy, entropy, inverse difference moment, and Haralick correlation) appeared to be good enough describers for vegetation texture for all bands (Fig. 4S). Then, the mean value of each attribute of each spectral band was extracted through segmented canopy polygons. Finally, a vegetated area is then characterized by 16 textural attributes (4 PS bands $\times$ 4 features).

The large view angle of the WV-2 sensor can generate an image displacement of tree crowns leading to a possible error source for identifying tree species (Pu and Landry, 2012). As the tree features can be affected by, for example, image resolution and environmental conditions at the time of acquisition (Beguet et al., 2014; Zhou et al., 2017), we tested three window sizes (3×3, 5×5, 10×10) with a fixed direction of 0∘ using the PAN band of the WV-2 image (Pu and Cheng, 2015). The window size 3×3 showed the best configuration for tree canopy texture.

2.3.6. *Training and validation samples*

The independent public tree inventories from both study areas were used as ground-truth samples (Fig. 2). From each municipal tree inventory, updated in July 2020, we selected dominant tree species, i.e., 22 in Aix-en-Provence and 20 in Florence, representing respectively 91.5% and 84.2% of the total number of inventoried public trees. Training samples were determined by the spatial join between the WV-2 imagery and the public tree inventory (Fig. 5S). We also included a class "grass" in training samples. We used 70% of the tree inventory data as training samples for the classification algorithm, and 30% for validation of classification. We defined 3,777 and 30,764 training samples in Aix-en-Provence and Florence, respectively. Finally, 16 texture-based features were extracted for each training sample and used as a reference

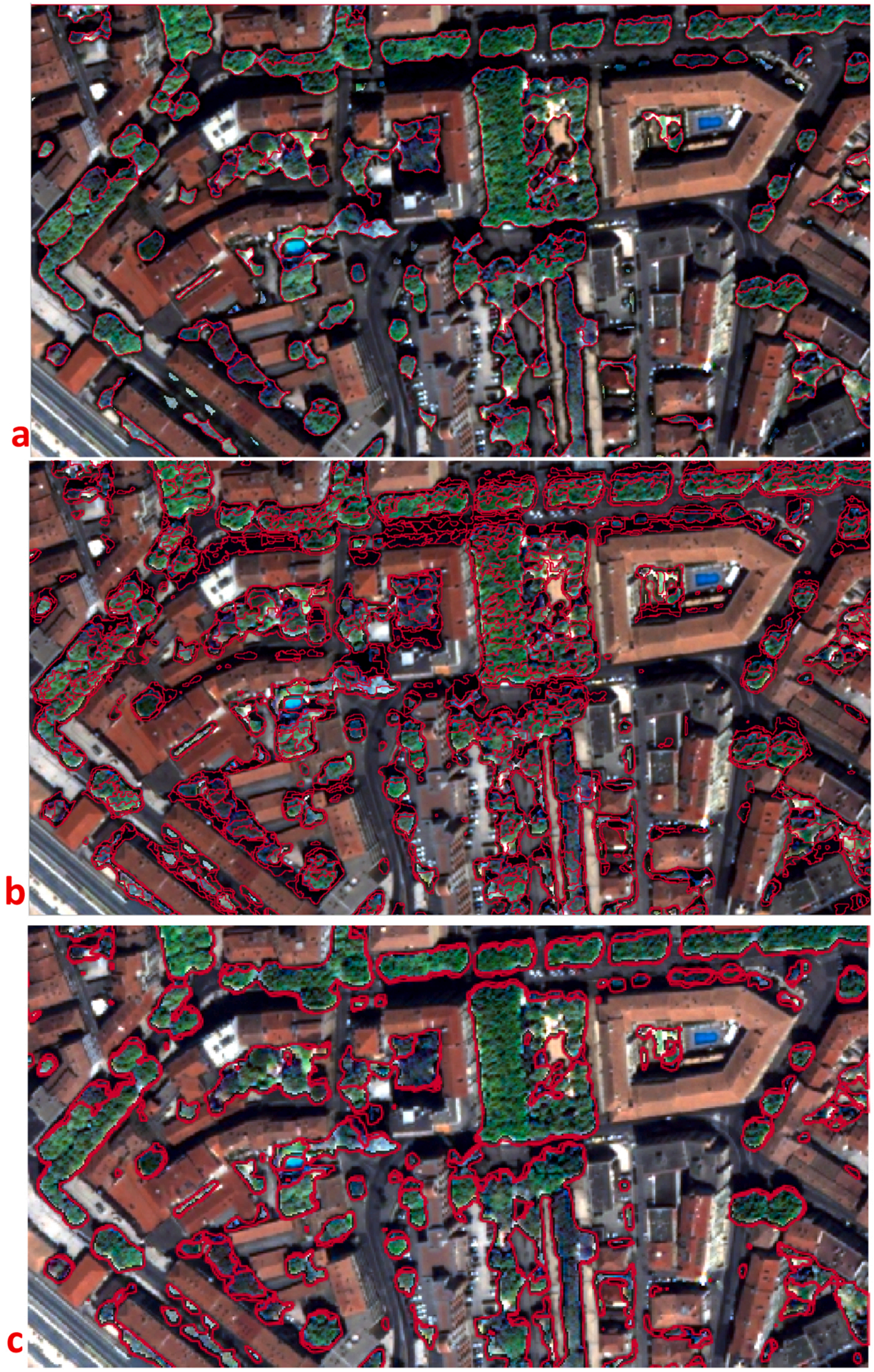

Fig. 4. Tree canopy segmentation - The watershed algorithm was used with different window sizes: e.g., 10 pixels and a range of 150 digital numbers (a); 10 pixels and a range of 100 digital numbers (b); and 20 pixels and a range of 250 digital numbers (c).

signature (Table 4S) for the object-based classification algorithm (Pu et al., 2011; Beguet et al., 2014; Choudhury et al., 2020).

2.3.7. Object-based classification

All the texture-based features were calculated over the study areas for 419,399 and 554,603 objects in Aix-en-Provence and Florence, respectively. For the assignment of objects to the different classes, i.e., plant species classification, the Random Forest (RF) classification algorithm (Breiman, 2001) was used using the reference signature (Table 4S) calculated from training samples (Genuer et al., 2010; Immitzer et al., 2012). Supervised RF classification is robust in separating classes by spectral properties (e.g., Immitzer et al., 2016; Belgiu and Drăguţ, 2016; Huesca et al., 2019). For each object, we retrieved the geographical coordinates (latitude, longitude) and the final class assignment (Fig. 6, Fig. 7).

2.3.8. Accuracy assessment

The quality of the object-based classification is evaluated through comparison to validation data representing the truth (also called "ground truth data"). To evaluate the results of the object-based classification, a confusion matrix was produced (Table 6S, Table 7S) and the Users, Producers, and overall accuracies as well as the Kappa coefficient

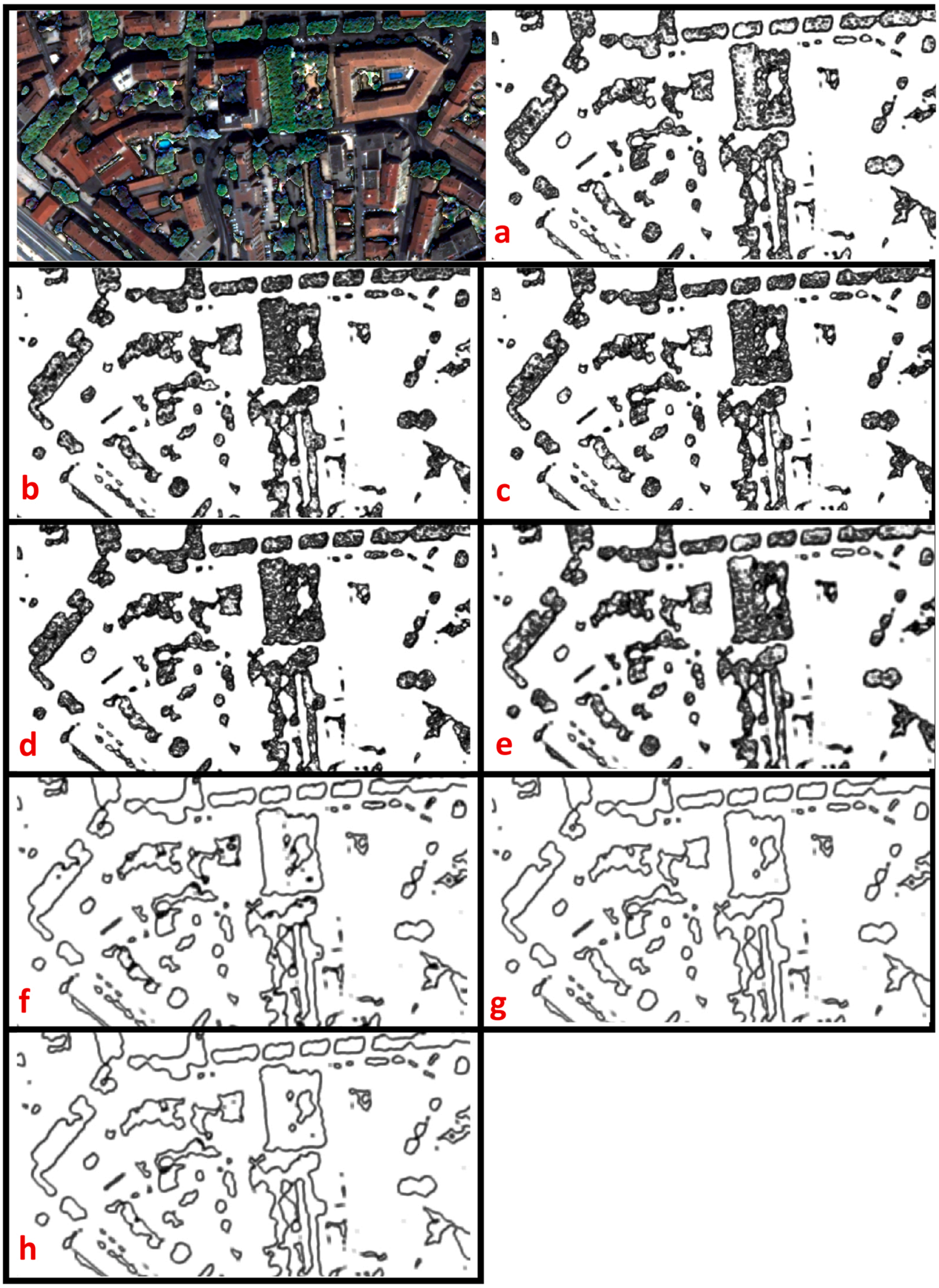

Fig. 5. Energy texture attribute for each band: coastal (a), blue (b), green (c), yellow (d), red (e), red-edge (f), near-infrared-1 (g), and near-infrared-2 (h).

were calculated for each class *c*. The procedure for accuracy measurement is based on the number of individual tree crowns and herbaceous areas assigned correctly to the different classes. The User's Accuracy represents class-wise accuracies from the point of view of the map user. The User's Accuracy provides the map user with a probability that a particular map location of class *c* is also the same class *c* in truth. The Producer's Accuracy represents class-wise accuracies from the point of view of the map maker.

$$Useraccuracy = \frac{Numberofcorrectlyclassifiedsamplesofclassc}{Numberofsamplesclassifiedasclassc}$$

$$Produceraccuracy = \frac{Numberofcorrectlyclassifiedsamplesofclassc}{Sumofsampleswithtrueclassc}$$

The overall accuracy represents the proportion of correctly classified samples (Braga et al., 2020).

$$Overallaccuracy = \frac{Numberofcorrectlyclassifiedsamples}{Numberofsamples}$$

The Kappa coefficient is generated to evaluate the accuracy of a classification. Kappa essentially evaluates how well the classification performed as compared to just randomly assigning values, i.e., did the classification do better than random. The Kappa Coefficient can range

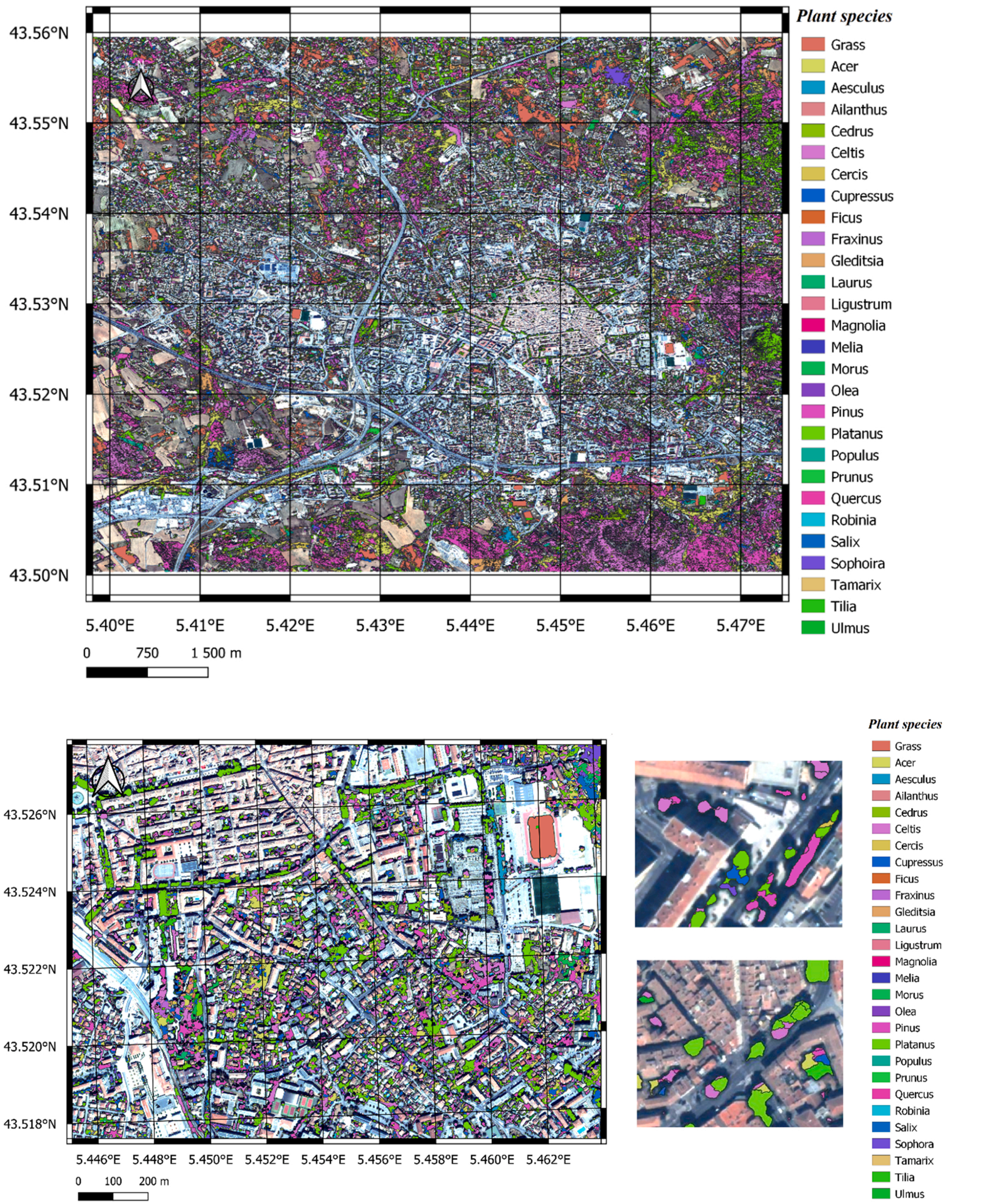

Fig. 6. . Detection, delineation, and classification of urban vegetation over the study area in Aix-en-Provence (top, 50 km^2) and a zoom over the south-east part of the study area (bottom).

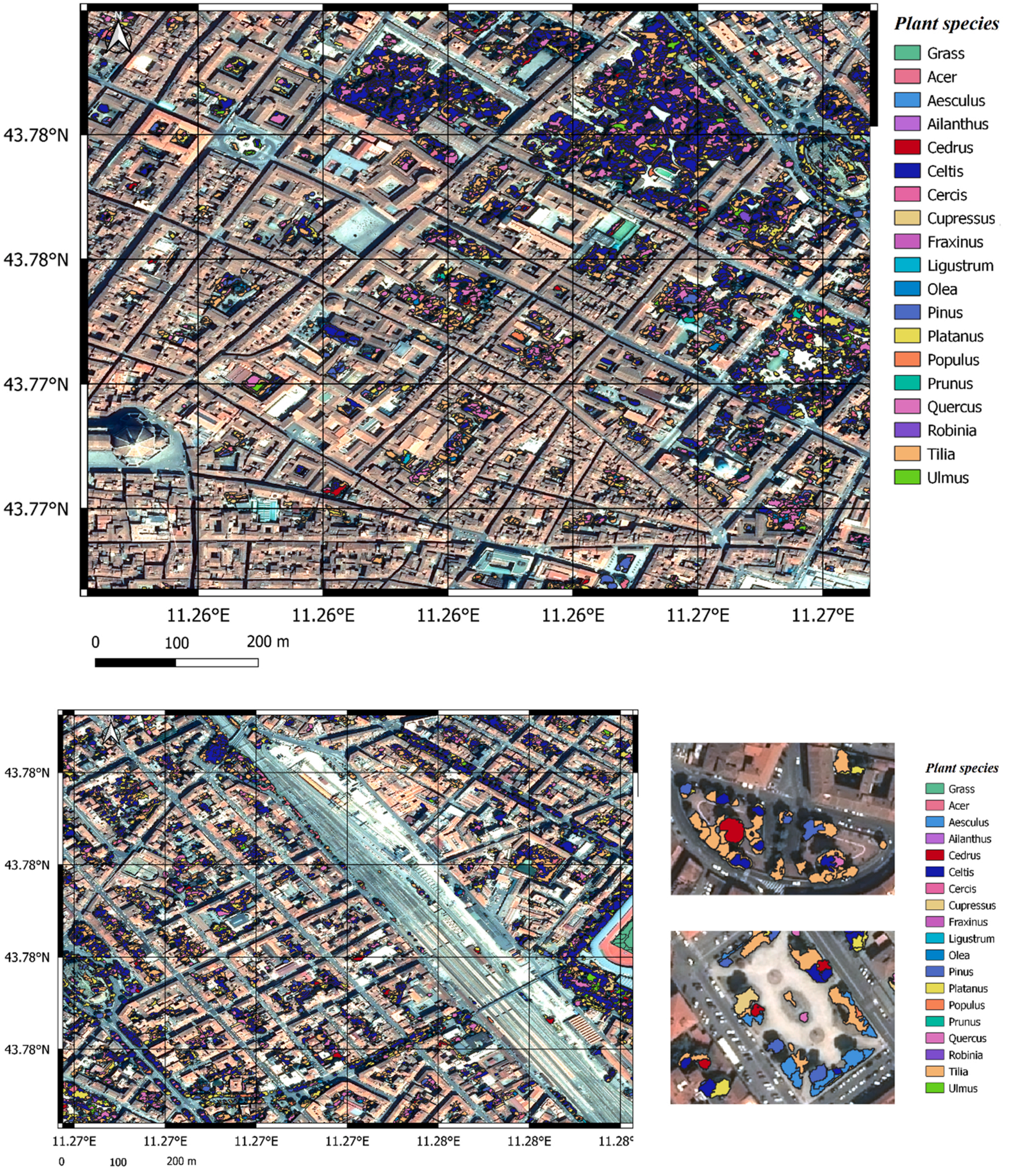

Fig. 7. Detection, delineation, and classification of urban vegetation over the study area in Florence: a zoom over the city center (top) and over the east part of the study area (bottom).

from -1 to 1. A value close to 1 indicates that the classification is significantly better than random (Braga et al., 2020).

$$k = \frac{po - pe}{1 - pe}$$

where p_o represents the actual observed agreement, and p_e represents chance agreement.

3. Results and discussion

In the present study, given the very-high spatial and spectral resolutions (e.g., PAN band at < 0.5 m resolution) and additional bands, we examined the suitability of WV-2 satellite imagery to identify urban vegetation in both private and public areas, and map the green cover by differentiating woody and herbaceous components over two large study areas in Aix-en-Provence and Florence. The images are of excellent quality, i.e., < 2% of the area is covered by clouds or haze. A pan-sharpening approach and stepwise masking protocol from WV-2 imagery were used to separate vegetated and non-vegetated areas, tree, and non-tree canopy, over the study areas prior to tree species mapping. The shadows of the trees, but also the shadows of the objects (e.g., buildings) were correctly removed in particular within residential yards. Then, we performed a MS procedure of object-based classification using RF classifier with different textural features extracted from tree canopy and grassland (lawn/turf) to identify and map dominant types of vegetation. As the NDVI of grass can be similar (or nearby) NDVI of a tree crown, the textural feature was effective in separating the tree canopies from grass/lawn.

The municipal tree inventories, based on field observations and mapped in a GIS, include only public trees managed by the municipality which represent e.g., about 7-14% of the total number of tree canopies detected in both public and private areas over the study areas in Florence (549,416 tree canopies detected and classified) and Aix-en-Provence (413,895 tree canopies detected and classified), respectively (Table 2, Table 3). Over both study areas, we also detected 1,157 and 5,438 herbaceous areas in Florence and Aix-en-Provence, respectively. The number of canopies not classified is very low, i.e., 66 out of 419,399 canopies were not classified in Aix-en-Provence (< 0.02%) and 4,030 out of 554,603 canopies in Florence (< 0.7%). In both study areas, about 85% of detected and classified tree canopies are in private lands. To date, city authorities use the inventory of trees in public areas, without access to the trees in private areas, to establish urban greening programs and carbon footprint. For the record, public officers are forbidden to enter in private and residential areas without formal authorization of owners, or without a search warrant. Such hindrance is unacceptable for a complete diagnosis of the carbon footprint, and precise calculation of the greenhouses gases and air pollutants absorbed by the urban trees; it hampers the development of a suitable and fit-for-purpose reforestation plan.

In Aix-en-Provence, the total canopy cover of most common tree species (Fig. 6, Table 2) are: *Pinus spp.* (~ 487 ha), *Celtis australis* (~ 374 ha), *Platanus acerifolia* (~ 370 ha), *Acer* spp. (~ 265 ha), *Cupressus sempervirens* (~ 124 ha), *Sophora japonica* (~ 54 ha), *Fraxinus spp.* (~ 41 ha), *Cercis siliquastrum* (~ 14 ha), *Populus* spp. (~ 8 ha), and *Tilia* spp. (~ 7 ha). In addition, the grass (lawn/turf) covers about 152 ha. The vegetated areas (trees and grass, Fig. 6S) cover 39.6% of the total WV-2 image area (i.e., 50 km^2) and this image area is 26.9% of the total city area. The overall accuracy for classifying 22 tree species and grass was around 84% with Kappa = 0.82 (Table 2). The producer's accuracies ranged from 55.6% (*Tamarix tetrandra*) to 96.1% (*Tilia spp.*). High classification accuracy (UA > 90%) was obtained for *Pinus spp.* (94.3%), *Platanus acerifolia* (93.6%), Grass (92.3%), *Sophora japonica* (91.8%), and *Cupressus sempervirens* (90.0%). The lowest classification accuracy (UA < 55%) was obtained for *Ulmus spp.* (54.1%) and *Quercus spp.* (46.6%).

Table 2
Results of accuracy of object-based classification performed from 3,777 training samples over the study area in Aix-en-Provence (50 km^2) based on four visible bands and four Haralick texture attributes: Number of tree canopies / herbaceous areas detected, Coverage (hectare), Kappa coefficient (k), producer accuracy (%), user accuracy (%), and overall accuracy (%) for 22 plant species and grass (lawn/turf) representing 91.5% of the total number of public trees inventoried in the municipal tree inventory. The ten most common tree species, accounting for about 75% of all public trees, are in bold.

Plant species	Number of tree canopies / grass areas classified	Coverage (ha)	No. of training samples	Producer accuracy (%)	User accuracy (%)
***Acer* spp.** [1]	**53,937**	**264.90**	**372**	**76.4**	**89.1**
Aesculus hippocastanum	157	3.37	51	87.8	81.8
Ailanthus altissima	70	0.82	35	65.7	74.2
Cedrus spp. [2]	800	7.20	54	87.3	73.8
Celtis australis	**104,625**	**373.73**	**381**	**84.1**	**82.1**
Cercis siliquastrum	**1,768**	**14.06**	**91**	**77.5**	**56.2**
Cupressus sempervirens	**38,761**	**124.21**	**343**	**81.2**	**90.0**
***Fraxinus* spp.** [3]	**2,407**	**40.94**	**125**	**74.9**	**72.0**
Gleditsia triacanthos	6,283	51.76	117	84.2	84.3
Laurus nobilis	11	0.26	15	64.7	85.7
Ligustrum japonicum	26	0.28	35	82.4	59.2
Morus nigra	801	7.26	115	73.2	85.0
***Pinus* spp.** [4]	**106,835**	**487.25**	**547**	**78.7**	**94.3**
Platanus acerifolia	**74,088**	**369.87**	**795**	**89.0**	**93.6**
***Populus* spp.** [5]	**701**	**8.37**	**75**	**86.8**	**61.1**
Prunus cerasifera	204	4.27	57	90.0	64.6
Quercus spp. [6]	87	5.91	32	83.9	46.6
Robinia pseudoacacia	65	0.75	38	90.6	62.5
Sophora japonica	**18,520**	**54.40**	**287**	**84.0**	**91.8**
Tamarix tetrandra	184	2.01	18	55.6	83.3
***Tilia* spp.** [7]	**3,370**	**7.14**	**75**	**96.1**	**74.5**
Ulmus spp. [8]	195	0.78	27	70.8	54.1
Grass	5,438	151.67	92	91.3	92.3
Not classified	66	0.70			
Total	**419,399**	**1981.91**	**3,777**		
Kappa coefficient (k)	**0.82**				
Overall accuracy (%)	**84.3**				
Green cover (%)	**39.6**				

1 Acer campestre, A. platanoides.
[2] Cedrus atlantica, C. deodara, C. libani.
[3] Fraxinus angustifolia, F. excelsior.
4 Pinus halepensis, P. pinaster, P. pinea.
5 Populus nigra, P. alba.
6 Quercus ilex, Q. pubescens, Q. cerris.
7 Tilia cordata, T. platyphyllos.
8 Ul*mus* campestris, U. minor.

Table 3
Results of accuracy of object-based classification performed from 30,764 training samples over the study area in Florence (80 km^2) based on four visible bands and four Haralick texture attributes: Number of detected tree canopies / herbaceous areas, Coverage (hectare), Kappa coefficient (k), producer accuracy (%), user accuracy (%), and overall accuracy (%) for 20 plant species and grass (lawn/turf) representing 84.2% of the total number of public trees inventoried in the municipal tree inventory. The ten most common tree species, accounting for approximately 65% of all public trees, are in bold.

Plant species	Number of tree canopies / grass areas classified	Canopy cover (ha)	No. of training samples	Producer accuracy (%)	User accuracy (%)
***Acer* spp.** [1]	**11,018**	**61.53**	**1,239**	**99.0**	**72.6**
Aesculus hippocastanum	774	4.20	323	99.1	65.7
Ailanthus altissima	272	1.01	81	100	71.1
Cedrus spp. [2]	3,768	17.93	726	100	85.6
Celtis australis	**107,677**	**337.93**	**5,227**	**66.3**	**91.4**
Cercis siliquastrum	717	2.94	233	100	76.9
Cupressus sempervirens	**54,403**	**175.75**	**1,828**	**97.8**	**91.8**
Fraxinus spp. [3]	2,652	20.46	672	99.6	72.8
Ligustrum spp. [4]	1,034	3.22	397	99.7	80.3
Magnolia grandiflora	102	0.67	32	96.9	63.3
Olea europaea	**22,462**	**87.67**	**1,172**	**76.5**	**67.5**
***Pinus* spp.** [5]	**39,723**	**277.70**	**2,033**	**94.7**	**89.6**
Platanus acerifolia	**23,456**	**89.65**	**2,443**	**99.0**	**85.7**
Populus spp. [6]	7,402	43.34	952	99.2	**79.5**
Prunus spp. [7]	1,702	6.63	544	99.6	71.3
***Quercus* spp.** [8]	**155,019**	**727.94**	**6,169**	**62.7**	**90.4**
Robinia pseudoacacia	**1,106**	**8.65**	**563**	**100**	**67.2**
Tilia europaea	**104,234**	**492.51**	**4,836**	**91.0**	**88.1**
***Ulmus* spp.** [9]	**11,895**	**47.47**	**1,283**	**88.1**	**64.7**
Grass	1,157	1.94	11	100	52.4
Not classified	4,030	18.66			
Total	**554,603**	**2427.16**	**30,764**		
Kappa coefficient (k)	**0.80**				
Overall accuracy (%)	**83.2**				
Green cover (%)	**30.3**				

1 Acer campestre, A. negundo, A. platanoides.
2 Cedrus atlantica, C. deodara.
3 Fraxinus angustifolia, F. excelsior.
4 Ligustrum japonicum, L. lucidum.
5 Pinus pinea, P. nigra.
6 Populus canescens, P. nigra, P. alba.
7 Prunus cerasifera, P. avium.
8 Quercus ilex, Q. robur, Q. rubra.
9 Ulmus campestris, U. minor.

In Florence, the total canopy cover of most common tree species (Fig. 7, Table 3) are: *Quercus* spp. (~ 728 ha), *Tilia europaea* (~ 492 ha), *Celtis australis* (~ 338 ha), *Pinus* spp. (~ 278 ha), *Cupressus sempervirens* (~ 176 ha), *Platanus acerifolia* (~ 90 ha), *Olea europaea* (~ 88 ha), and *Acer* spp. (~ 61 ha). The grass covers about 2 ha, this low surface area is likely due to dry conditions during satellite image acquisition (30 July 2020), when the grass is less green, and the NDVI masking did not class the pixels as vegetated areas. The vegetated areas cover 30.3% of the total WV-2 image area (i.e., 80 km^2) and this image area is 78.4% of the total city area. In this study, for classifying 20 tree species and grass, the overall accuracy was around 83% with Kappa = 0.80 (Table 3). The Producer's Accuracies ranged from 62.7% (*Quercus* spp.) to 100% for several species (*Ailanthus altissima, Cedrus* spp.*, Cercis siliquastrum, Magnolia grandiflora, Robinia pseudoacacia*, and grass). High classification accuracy (UA > 90%) was obtained for *Cupressus sempervirens* (91.8%), *Celtis australis* (91.4%), *and Quercus* spp. (90.4%). The lowest classification accuracy was obtained for grass (52.4%), and for *Magnolia grandiflora* (63.3%) and *Ulmus* spp. (64.7%).

The calculation of attributes from the additional WV-2 bands improved the overall accuracy for identifying plant species, e.g., from 58% to 63% for seven tree species (Pu and Landry, 2012). In this study, the quality and accuracy of the object-based classification was higher (Table 5S) by using four bands and four texture features (overall accuracy 84%, Kappa 0.82) than eight bands and ten texture features (overall accuracy 74%, Kappa 0.72), when we classified more than 20 dominant plant species. Therefore, we used four spectral bands (blue, green, yellow, red), and four texture features (i.e., energy, entropy, inverse difference moment, Haralick correlation) which were selected as the most efficient texture-based attributes for plant species classification from WV-2 images. By including the four additional WV-2 bands (coastal, yellow, red edge, and near infrared 2) in the set of explanatory variables, the number of variables used in the classification is doubled. From this, we expected a strong effect on classification accuracy while in our study, a negative effect on classification accuracy was observed, and can be explained by the pairwise band correlations (Immitzer et al., 2012). Adding four new bands to the four standard bands introduced a lot of redundant information and unvaluable information to descriptors variables for machine learning and therefore reduce the classification accuracy. From this, we concluded that the additional bands play only a minor part in urban plant species classification. Immitzer et al. (2012) deeply investigated all four-band combinations, and the best classification results were obtained with band combinations including at least three standard bands.

The lowest classification accuracy is mainly due the low number of training samples, e.g., for *Quercus* spp. and *Ulmus* spp. in Aix-en-Provence, and grass and *Magnolia grandiflora* in Florence. For these tree species it was difficult to find reliable reference samples in urban settings, as they usually do not occur in pure stands. Some of misclassifications are likely due to errors in the reference data set. Hartling et al. (2019) have tested the effect of the number training samples on classifier performance and have suggested to select tree species with more than 100 ground truth samples collected within the study area. The low classification accuracy can be also due to the small crown diameter (< 3 m) and/or varying reflectance of canopies, and their background, such as understory and soil. Previously, the WV-2 spatial resolution was also insufficient to capture all pixels of the whole Magnolia crown (Pu and Landry, 2012). Due to similar geometric and physiognomic characteristics, the leaves and canopies of *Quercus* spp. produced a similar spectral signature across wavelengths 400-2400 nm (Pu, 2009). For the same tree species, variations in the reflectance within the canopy can be due to soil characteristics (Key et al., 1998), age differences between leaves within the crown (Blackburn and Milton, 1995), and many other environmental factors (Pu, 2009).

The object-oriented image analysis, based on spectral and textural attributes from WorldView-3 (WV-3) images, was applied for urban tree species identification and mapping in Northern Italy (Choudhury et al., 2020). Due to spectral similarities, they detected four tree species in an urban park (*Acer campestre; Platanus* spp.*; Populus nigra; Quercus* spp.) and three species in some streets (*Platanus* spp.*; Quercus* spp.*, Tilia platyphyllos*). The overall accuracy was 78%, with UA ranging from 52% for *Tilia platyphyllos* to 97% for *Platanus* spp. in the streets (Choudhury et al., 2020). In our study, these tree species were classified at city scale in Florence, center of Italy, with a higher overall accuracy of 83%. We obtained similar UA for *Populus* sp. (~79%), higher UA for *Platanus* spp. in parks (86% vs. 73%), for *Tilia platyphyllos* (88% vs. 52%), and *Quercus* spp. in the streets (90% vs. 55%), while lower UA were obtained for *Acer campestre* (73% vs. 81%) and *Platanus* spp. in the streets (86% vs. 97%). Li et al. (2015) used WV-2 images for identifying five tree species (*Paulownia tomentosa*, *Populus tomentosa*, *Sophora Japonica*, *Ginkgo biloba* and *Platanus acerifolia*) with the object-based RF classifier in two study areas in Beijing (China). The overall accuracy was 77% in Capital Normal University and of 71% in Beijing Normal University (Li et al., 2015). In Aix-en-Provence and Florence, we obtained higher UA for *Sophora Japonica* (92% vs. 60-73%) and *Platanus acerifolia* (86-94% vs. 80%) and quite similar for *Populus* spp. (61-80 vs. 81-70%). Pu and Landry (2012) investigated the potential of WV-2 images for mapping seven urban tree species (*C. camphora, M. grandiflora, Q. geminata, Q. laurifolia, Q. virginiana, Palmae* sp., and *Pinus* sp.) over a study area in the city of Tampa (United States). By using the sunlit training samples, the overall accuracy was low (57%) mainly due to similar characteristics of leaves and canopies and similar spectral signature of oak species (Pu and Landry, 2012). Both *Palmae sp.* and *M. grandiflora* produced a very low accuracy (< 35%). In our study, a higher overall accuracy was obtained in both urban areas (over 83%) as well as higher UA for *Pinus* spp. (90-94% vs. 86%), for *Quercus* spp. (47-90% vs. 51-75%), and *M. grandiflora* (63% vs. 36%).

Tigges et al. (2013) explored the identification of eight tree species (*Acer* sp., *Aesculus* sp.*, Fagus sylvatica*, *Pinus sylvestris, Platanus* spp.*, Populus* sp.*, Quercus* sp., and *Tilia* sp.) in some streets in Berlin (Germany) using RapidEye imagery, with an overall accuracy of 85%, similar to our study. In our study, we obtained similar UA for *Acer* sp. (73-89% vs. 86%), *Pinus* sp. (90-94% vs. 99%), *Platanus* spp. (86-94% vs. 93%), *Quercus* spp. (47-90% vs. 66%), and *Tilia* sp. (74-88% vs. 78%), and lower UA for *Aesculus* sp. (66-82% vs. 99%) and *Populus* sp. (61-80% vs. 88%). Pu et al. (2011) identified five types of vegetation from IKONOS imagery within the City of Tampa. The class-specific accuracies are similar to our UA, i.e., about 90% for broadleaf trees, while they reported 74% for grass/lawn (Pu et al., 2011) much lower than the UA calculated in Aix-en-Provence (UA = 92%). Ke et al. (2010) used object-based approach with QuickBird imagery to classify trees into 5 categories with a low overall accuracy of 66% over a study area nearby New York.

4. Conclusions

Green spaces within private areas provide important contributions to the sustainability of urban systems. Despite that private areas occupy a large proportion of cities; domestic gardens and private areas are seldom included in the development and management of urban greening programs by local authorities to generate and sustain urban biodiversity while the trees in private areas amount to about 85% of the trees' population in cities. For urban climate change resilience, it is essential to identify the dominant tree species and map the canopy cover in both public and private areas to quantify the environmental benefits of urban trees e.g., air pollution and carbon mitigation, islands of freshness, but also socio-economic benefits (e.g., physical, mental, and social well-being).

In forestry and city-planning, the detection of individual tree crown, and investigating the trees characteristics and diversity within private areas, from VHR imagery is a challenging field of research to make a realistic inventory of urban trees and quantitative analysis. Compared with street trees in public areas, acquisition of reliable information on trees characteristics in private land and courtyards is lacking mainly due to access restrictions, complex spatial structure and landscape patterns, with building and shadows presence, and high plant species diversity in private residential gardens (lots of non-native ornamental species).

In this study, a object-based classification was applied for detecting, delineating, and identifying plant species in urban areas from very-high resolution image (i.e., WorldView). The methodology consisted of six steps: 1) Preprocessing of the WV-2 imagery; 2) Stepwise masking system using the threshold of NDVI to separate the study area into vegetated and non-vegetated areas; 3) Image segmentation into polygons representing each vegetated area (tree crown and grass); 4) Texture-based features extraction from a GLCM; 5) Extracting training samples with references to ground survey data; and 6) using RF classifier to identify and map urban plant species. Based on spectral and textural differences between vegetated and non-vegetated areas, and between herbaceous areas (lawn/turf) and tree canopies, all tree species were classified.

We demonstrated the robustness and effectiveness of satellite imagery at very-high spectral and spatial resolution, such as WV-2 (50 cm in PAN, 2 m in MS mode), for identifying, delineating, and classifying more than 20 dominant plant species and herbaceous areas in urban environment such as roads, parks, and open courtyards in private areas over two large cities (50-80 km^2) in France and Italy with an overall accuracy for classifying tree species over 83%. In both study areas, about 420,000 and 555,000 canopies were successfully classified in Aix-en-Provence and Florence with about 85% in private lands and not under municipalities supervision.

High classification accuracy was obtained for *Pinus* spp. (94.3%), *Platanus acerifolia* (93.6%), grass (92.3%), and *Sophora japonica* (91.8%) in Aix-en-Provence, and for *Cupressus sempervirens* (91.8%), *Celtis australis* (91.4%), *Quercus* spp. (90.4%), and *Pinus* spp. (89.6%) in Florence. The relatively high classification accuracies are mainly due to the spectral and spatial properties of the WV-2 sensor, suitable for plant species classification, as well as suitability of tree crown spectral and textural descriptors, and a consistent learning and test datasets. Due to spatial proximity between tree canopies along boulevard, in parks and cemeteries, the crown segmentation step is fundamental to overcome the most challenging part of tree species classification in urban environment. The classification of crown objects, as an average over a couple of pixels, rather than individual pixels captures species-specific differences in crown structure and transmissivity in various spectral bands. By focusing on dominant tree species, and by considering the sunlit regions of the tree crowns in the classification process, have contributed to high classification accuracies. The low accuracy for identifying some urban tree species e.g., *Quercus* spp. and *Magnolia grandiflora* is likely due to i) the low number of training sample available for the species from municipality tree inventories; and ii) to canopy spectral similarity among tree species. Large sample size per class, with more than 100 ground truth samples, certainly had a positive impact on the overall classification results.

Accurate data on tree distribution, tree species and structural characteristics of trees within the city are currently obtained by visual field observations, which are costly and time-consuming (e.g., in Aix-en-Provence with about 5,000 trees per km^2, it would take around 1,000 hours of field investigation, i.e., more than 0.5 man per year per km^2). The use of remote sensing techniques for urban tree species mapping ensures significant time savings compared to the traditional tree observations within a territory. With our approach a full tree inventory mapped in a GIS, gathering all dominant trees in both private and public areas, can be provided to municipalities to implement an efficient Urban Greening Plan in the framework of the EU Biodiversity Strategy for 2030 (for cities of at least 20,000 inhabitants) and to assess their Carbon footprint at city scale. Such a quick inventory technique has the potential to be frequently repeated to monitor changes over time.

This study provided a strong baseline to proceed with classification and mapping of plant species in urban areas by use of remote sensing techniques to compliment not replace the traditional methods and to take into account private lands green infrastructures in the inventory of tree heritage in cities. The proposed methodology is an efficient tool to assist urban planners and environmental policymakers in planning suitable greening strategies and urban air quality assessments.

CRediT authorship contribution statement

Conceptualization, P.S., F.C., and E.P.; methodology, P.S. and F.C.; data curation, P.S., M.L. and F.C.; writing - original draft, P.S. and F.C.; writing - review & editing, P.S., J.M., Y.H., V.A., A.D.M., and E.P.; supervision, P.S. All authors have read and agreed to the published version of the manuscript.

Declaration of Competing Interest

The authors declare that they have no known competing financial interests or personal relationships that could have appeared to influence the work reported in this paper.

Acknowledgments

This work was carried out with the contribution of the LIFE financial instrument of the European Union (LIFE19 ENV/FR/000086) in the framework of the AIRFRESH project "*Air pollution removal by urban forests for a better human well-being*", and the Research Council of Lithuania (agreement No. S-LZ-21-3), and the Franco-Lithuanian Programme Hubert Curien (PHC) GILIBERT 2021 (46429UB). Project funded under the National Recovery and Resilience Plan (NRRP), Mission 4 Component 2 Investment 1.4 - Call for tender No. 3138 of 16 December 2021, rectified by Decree n.3175 of 18 December 2021 of Italian Ministry of University and Research funded by the European Union – Next Generation EU. Project code CN_00000033, Concession Decree No. 1034 of 17 June 2022 adopted by the Italian Ministry of University and Research, CUP B83C22002930006, Project title "National Biodiversity Future Center - NBFC".

Appendix A. Supporting information

Supplementary data associated with this article can be found in the online version at doi:10.1016/j.ufug.2023.127866.

References

Adam, E., Mutanga, O., Odindi, J., Abdel-Rahman, E.M., 2014. Land-use/cover classification in a heterogeneous coastal landscape using RapidEye imagery: Evaluating the performance of random forest and support vector machines classifiers. Int. J. Remote Sens. 35, 3440–3458.
Akbari, H., Kalbi, S., 2016. Determining Pleiades satellite data capability for tree diversity modeling. iForest 10, 348–352.
Alonzo, M., McFadden, J.P., Nowak, D.J., Roberts, D.A., 2016. Mapping urban forest structure and function using hyperspectral imagery and lidar data. Urban For. Urban Green 17, 135–147.
Alonzo, M., Bookhagen, B., McFadden, J.P., Sun, A., Roberts, D.A., 2015. Mapping urban forest leaf area index with airborne lidar using penetration metrics and allometry. Remote Sens. Environ. 162, 141–153.
Anenberg, S.C., Mohegh, A., Goldberg, D.L., Kerr, G.H., Brauer, M., et al., 2022. Long-term trends in urban NO_2 concentrations and associated paediatric asthma incidence: estimates from global datasets. Lancet Planet Health 6, e49–e58.
Baró, F., Haase, D., Gómez-Baggethun, E., Frantzeskaki, N., 2015. Mismatches between ecosystem services supply and demand in urban areas: a quantitative assessment in five European cities. Ecol. Indic. 55, 146–158.
Beguet B., Chehata N., Boukir S., Guyon D., 2014, "Classification of forest structure using very high-resolution Pleiades image texture". Conference Paper IGARSS July 2014.
Belgiu, M., Drăguţ, L., 2016. Random Forest in remote sensing: A review of applications and future directions. ISPRS J. Photogramm. Remote Sens. 114, 24–31.
Blackburn, G.A., Milton, E.J., 1995. Seasonal variations in the spectral reflectance of deciduous tree canopies. Int. J. Remote Sens. 16, 709–720.
Blaschke, T., 2010. Object based image analysis for remote sensing. ISPRS J. Photogramm. Remote Sens. 65, 2–16.
Bottalico, F., Travaglini, D., Chirici, G., Garfì, V., Giannetti, F., et al., 2017. A spatially-explicit method to assess the dry deposition of air pollution by urban forests in the city of Florence, Italy. Urban For. Urban Green. 27, 221–234.
Boukir S., Regniers O., Guo L., Bombrun L., Germain C., 2015, "Texture-based forest cover classification using random forests and ensemble margin". IEEE International Geoscience and Remote Sensing Symposium 2015, Milan, Italy. Pp. 3072–3075.
Bovolo, F., Bruzzone, L., Capobianco, L., Garzelli, A., Marchesi, S., 2010. Analysis of effect of pan-sharpening in change detection on VHR Images. IEEE Trans. Geosci. Remote Sens. Lett. 7, 53–57.
Braga, J.R.G., Peripato, V., Dalagnol, R., Ferreira, M.P., Tarabalka, Y., et al., 2020. Tree crown delineation algorithm based on a convolutional neural network. Remote Sens 12, 1288.
Breiman, L., 2001. Random forests. Mach. Learn 45, 5–32.
Cameron, R.W.F., Blanuša, T., Taylor, J.E., Salisbury, A., Halstead, A.J., et al., 2012. The domestic garden: Its contribution to urban green infrastructure. Urban For. Urban Green. 11, 129–137.
Chavez Jr., P.S., 1988. An improved dark-object subtraction technique for atmospheric scattering correction of multispectral data. Remote Sens. Environ. 24, 459–479.
Chen G., Ozelkan E., Singh K.K., Zhou J., Brown M.R., 2017, "Meentemeyer, R.K. Uncertainties in Mapping Forest Carbon in Urban Ecosystems". J. Environ. Manag. 187: 229–238.
Choudhury, M.A.M., Marcheggiani, E., Despini, F., Costanzini, S., Rossi, P., et al., 2020. Urban tree species identification and carbon stock mapping for urban green planning and management. Forests 11, 1226.
Choudhury M.A.M., Costanzini S., Despini F., Rossi P., Galli A., et al., 2019, "Photogrammetry and Remote Sensing for the identification and characterization of trees in urban areas". IOP Conf. Series: Journal of Physics: Conf. Series 1249: 012008.
Cilliers, S., Siebert, S., Davoren, E., Lubbe, R., 2012. Social aspects of urban ecology in developing countries, with an emphasis on urban domestic gardens. Appl. Urban Ecol.: A Glob. Framew. 123–138.
Deur, M., Gašparović, M., Balenović, I., 2020. Tree species classification in mixed deciduous forests using very high spatial resolution satellite imagery and machine learning methods. Remote Sens 12, 3926.
Effiom A.E., 2018, "UAV-RGB and Multispectral Pleiades images for tree species identification and forest carbon estimation in Amtsvenn, Germany". PhD thesis, Faculty of Geo-Information Science and Earth Observation of the University of Twente, February 2018, 63 pp.
European Union Biodiversity Strategy for 2030 "Bringing nature back into our lives" (COM(2020) 380 final), Brussels, 20.5.2020.
Fusaro, L., Marando, F., Sebastiani, A., Capotorti, G., Blasi, C., et al., 2017. Mapping and assessment of PM_{10} and O_3 removal by woody vegetation at urban and regional level. Remote Sens 9, 791.
Galle, N.J., Halpern, D., Nitoslawski, S., Duarte, F., Ratti, C., Pilla, F., 2021. Mapping the diversity of street tree inventories across eight cities internationally using open data. Urban For. Urban Green. 61, 127099.
Genuer, R., Poggi, J.M., Tuleau-Malot, C., 2010. Variable selection using random forests. Pattern Recognit. Lett. 31, 2225–2236.
Grote, R., Samson, R., Alonso, R., Amorim, J.U., Calfapietra, C., et al., 2016. Functional traits of urban trees in relation to their air pollution mitigation potential: a holistic discussion. Front. Ecol. Environ. 1–8.
Hartling, S., Sagan, V., Sidike, P., Maimaitijiang, M., Carron, J., 2019. Urban tree species classification using a WorldView-2/3 and LiDAR data fusion approach and deep learning. Sensors 19, 1284.
Huesca, M., Roth, K.L., García, M., Ustin, S.L., 2019. Discrimination of Canopy Structural Types in the Sierra Nevada Mountains in Central California. Remote Sens 11, 1100.
Immitzer, M., Vuolo, F., Atzberger, C., 2016. First experience with sentinel-2 data for crop and tree species classifications in Central Europe. Remote Sens 8, 166.
Immitzer, M., Atzberger, C., Koukal, T., 2012. Tree species classification with random forest using very high spatial resolution 8-band WorldView-2 satellite data. Remote Sens. 4, 2661–2693.
Jones, E.G., Wong, S., Milton, A., Sclauzero, J., Whittenbury, H., McDonnell, M.D., 2020. The impact of pan-sharpening and spectral resolution on vineyard segmentation through machine learning. Remote Sens 12, 934.

Ke, Y., Quackenbush, L.J., Im, J., 2010. Synergistic use of QuickBird multispectral imagery and LIDAR data for object-based forest species classification. Remote Sens. Environ. 114, 1141–1154.

Key, T., Warner, T.A., McGraw, J.B., Fajvan, M.A., 2001. A comparison of multispectral and multitemporal information in high spatial resolution imagery for classification of individual tree species in a temperate hardwood forest. Remote Sens. Environ. 75, 100–112.

Key T., Warner T.A., McGraw J.B., Fajvan M.A., 1998, "An evaluation of the relative spectral and phenological information for tree canopy classification of digital images in the eastern deciduous forest," in Presentation in the Int. Forum on Automated Interpretation of High Spatial Resolution Digital Imagery for Forestry, Victoria, BC, Canada, Feb. 10–12, 1998, pp. 243–254.

Kizel F., Bruzzone L., Benediktsson J.A., 2017, "Simultaneous empirical line calibration of multiple spectral images". 2017 IEEE International Geoscience and Remote Sensing Symposium (IGARSS). doi:10.1109/igarss.2017.8127924.

Klingberg, J., Broberg, M., Strandberg, B., Thorsson, P., Pleijel, H., 2017. Influence of urban vegetation on air pollution and noise exposure - A case study in Gothenburg, Sweden. Sci. Total Environ. 599–600, 1728–1739.

Knauer, U., von Rekowski, C.S., Stecklina, M., Krokotsch, T., Pham Minh, T., et al., 2019. Tree species classification based on hybrid ensembles of a convolutional neural network (CNN) and random forest classifiers. Remote Sens 11, 2788.

Kokubu, Y., Hara, S., Tani, A., 2020. Mapping seasonal tree canopy cover and leaf area using worldview-2/3 satellite imagery: a megacity-scale case study in Tokyo urban area. Remote Sens 12, 1505.

Larondelle, N., Haase, D., Kabisch, N., 2014. Mapping the diversity of regulating ecosystem services in European cities. Glob. Environ. Chang. 26, 119–129.

Lefebvre, A., Nabucet, J., Corpetti, T., Courty, N., Hubert-Moy, L., 2016. Extraction of urban vegetation with Pléiades multi-angular images". Remote Sensing Technologies and Applications in Urban. Environ., Proc. SPIE Vol. 10008, 100080H.

Li, D., Ke, Y., Gong, H., Li, X., 2015. Object-based urban tree species classification using Bi-temporal WorldView-2 and WorldView-3 images. Remote Sens 7, 16917–16937.

Loram, A., Tratalos, J., Warren, P.H., Gaston, K.J., 2007. Urban domestic gardens (X): the extent and structure of the resource in five major cities. Landsc. Ecol. 22, 601–615.

Maack, J., Kattenborn, T., Fassnacht, F.E., Enßle, F., Hernández, J., et al., 2015. Modeling Forest biomass using Very-High-Resolution data - Combining textural, spectral and photogrammetric predictors derived from spaceborne stereo images. Eur. J. Remote Sens 48, 245–261.

Maes, J., Liquete, C., Teller, A., Erhard, M., Paracchini, M.L., et al., 2016. An indicator framework for assessing ecosystem services in support of the EU Biodiversity Strategy to 2020. Ecosyst. Serv. 17, 14–23.

Malashock, D.A., Delang, M.N., Becker, J.S., Serre, M.L., West, J.J., et al., 2022. Estimates of Ozone Concentrations and Attributable Mortality 1 in Urban, Peri-Urban and Rural Areas Worldwide in 2019. Environ. Res. Lett. 17, 054023.

Manes, F., Marando, F., Capotorti, G., Blasi, C., Salvatori, E., et al., 2016. Regulating ecosystem services of forests in ten Italian metropolitan 31 cities: Air quality improvement by PM_{10} and O_3 removal. Ecol. Indic. 67, 425–440.

Manes, F., Incerti, G., Salvatori, E., Vitale, M., Ricotta, C., Costanza, R., 2012. Urban ecosystem services: Tree diversity and stability of tropospheric ozone removal. Ecol. Appl. 22, 349–360.

Marando, F., Salvatori, E., Fusaro, L., Manes, F., 2016. Removal of PM_{10} by forests as a nature-based solution for air quality improvement in the metropolitan city of Rome. Forests 7, 1–14.

McPherson, E.G., van Doorn, N., de Goede, J., 2016. "Structure, Funct. Value Str. trees Calif., Usa". Urban For. Urban Green. 17, 104–115.

Modica, G., Solano, F., Merlino, A., Di Fazio, S., Barreca, F., et al., 2016. Using Landsat 8 Imagery in Detecting Cork Oak (Quercus suber L.). In: J. Agric. Eng, 47. A Case Study in Calabria (Italy), Woodlands, pp. 205–215.

Müller N., Werner P., Kelcey J.G., 2010, "Urban biodiversity and design". Conservation Science and Practice Series No. 7. Blackwell Publishing Ltd., Oxford, England. https://doi.org/10.1002/9781444318654.

Niccolai, A., Hohl, A., Niccolai, M., Oliver, C.D., 2010. Integration of varying spatial, spectral and temporal high-resolution optical images for individual tree crown isolation. Int. J. Remote Sens 31, 5061–5088.

Nichol, J., Wong, M.S., 2007. Remote sensing of urban vegetation life form by spectral mixture analysis of high-resolution IKONOS satellite images. Int. J. Remote Sens. 28, 985–1000.

Nouri, H., Beecham, S., Anderson, S., Nagler, P., 2014. High spatial resolution WorldView-2 imagery for mapping NDVI and its relationship to temporal urban landscape evapotranspiration factors. Remote Sens. 6, 580–602.

Nowak, D.J., Hirabayashi, S., Doyle, M., McGovern, M., Pasher, J., 2018. Air pollution removal by urban forests in Canada and its effect on air quality and human health. Urban For. Urban Green. 29, 40–48.

Nowak D.J., Hirabayashi S., Bodine A., Hoehn R., 2013, "Modeled PM2.5 removal by trees in ten US cities and associated health effects". Environ. Pollut. 178: 395–402.

Nowak, D.J., Crane, D.E., Stevens, J.C., Hoehn, R.E., Walton, J.T., Bond, J., 2008. A ground-based method of assessing urban forest structure and ecosystem services. Arboric. Urban For. 34, 347–358.

Ostberg, J., Wiström, B., Randrup, T.B., 2018. The state and use of municipal tree inventories in Swedish municipalities - Results from a national survey. Urban Ecosyst. 21. https://doi.org/10.1007/s11252-018-0732-3.

Owen J. 2010, "Wildlife of a garden: a thirty-year study". Royal Horticultural Society. Peterborough, Cambridgeshire, UK, ISBN-10: ‎ 9781907057120.

Pace, R., De Fino, F., Rahman, M.A., Pauleit, S., Nowak, D.J., Grote, R., 2021. A single tree model to consistently simulate cooling, shading, and pollution uptake of urban trees. Int. J. Biometeorol. 65, 277–289.

Pace, R., Biber, P., Pretzsch, H., Grote, R., 2018. Modeling ecosystem services for park trees: sensitivity of i-tree eco simulations to light exposure and tree species classification. Forests 9, 89.

Parmehr, E.G., Amati, M., Taylor, E.J., Livesley, S.J., 2016. Estimation of urban tree canopy cover using random point sampling and remote sensing methods. Urban For Urban Green. 20, 160–171.

Pataki, D.E., Carreiro, M.M., Cherrier, J., Grulke, N.E., Jennings, V., et al., 2011. Coupling biogeochemical cycles in urban environments: ecosystem services, green solutions, and misconceptions. Front. Ecol. Environ. 9, 27–36.

Pauleit, S., Jones, N., Nyhuus, S., Pirnat, J., Salbitano, F., 2005. Urban forest resources in European cities. In: Konijnendijk, C.C., Nilsson, K., Randrup, T.B., Schipperijn, J. (Eds.), Urban Forests and Trees. Springer, Berlin, Heidelberg, New York, pp. 49–80.

Persson, H.J., 2016. Estimation of boreal forest attributes from very high resolution pléiades data. Remote Sens 8, 736.

Pope, G., Treitz, P., 2013. Leaf area index (LAI) estimation in boreal mixed wood forest of Ontario, Canada using light detection and ranging (LiDAR) and worldview-2 imagery. Remote Sens 5, 5040–5063.

Pretzsch, H., Moser-Reischl, A., Rahman, M.A., Pauleit, S., Rötzer, T., 2021. Towards sustainable management of the stock and ecosystem services of urban trees. From theory to model and application. Trees. https://doi.org/10.1007/s00468-021-02100-3.

Proietti, C., Anav, A., De Marco, A., Sicard, P., Vitale, M., 2016. A multi-sites analysis on the ozone effects on Gross Primary Production of European forests. Sci. Total Environ. 556, 1–11.

Pu, R., 2011. Mapping urban forest tree species using IKONOS imagery: preliminary results. Environ. Monit. Assess. 172, 199–214.

Pu, R., 2009. Broadleaf species recognition within situ hyperspectral data. Int. J. Remote Sens. 30, 2759–2779.

Pu, R., Landry, S., 2019. Evaluating seasonal effect on forest leaf area index mapping using multi-seasonal high resolution satellite Pleiades imagery. Int. J. Appl. Earth Obs. Geoinf. 80, 268–279.

Pu, R.J., Cheng, J., 2015. Mapping Forest leaf area index using reflectance and textural information derived from WorldView-2 imagery in a mixed natural forest area in Florida, US. Int. J. Appl. Earth Obs. Geoinf. 42, 11–23.

Pu, R., Landry, S., Zhang, J., 2015. Evaluation of atmospheric correction methods in identifying urban tree species with WorldView-2 imagery. J. Sel. Top Appl. Earth Obs. Remote Sens. 8, 1886–1897.

Pu, R., Landry, S., 2012. A comparative analysis of high spatial resolution IKONOS and WorldView-2 imagery for mapping urban tree species. Remote Sens. Environ. 124, 516–533.

Pu, R., Landry, S., Yu, Q., 2011. Object-based urban detailed land cover classification with high spatial resolution IKONOS imagery. Int. J. Remote Sens. 32, 3285–3308.

Pu, R., Kelly, M., Anderson, G.L., Gong, P., 2008. Using CASI hyperspectral imagery to detect mortality and vegetation stress associated with a new hardwood forest disease. Photogramm. Eng. Remote Sens. 74, 65–75.

Puissant, A., Rougier, S., Stumpf, A., 2014. Object-oriented mapping of urban trees using random forest classifiers. Intern. J. Appl. Earth Obs. Geoinform. 26, 235–245.

Qian, Y., Zhou, W., Nytch, C.J., Han, L., Li, Z., 2020. A new index to differentiate tree and grass based on high resolution image and object-based methods. Urban For. Urban Green. 53, 126661.

Quackenbush, L.J., Hopkins, P.F., Kinn, G.J., 2000. Developing forestry products from high resolution digital aerial imagery. Photogramm. Eng. Remote Sens. 66, 1337–1346.

Rahman, M.A., Hartmann, C., Moser-Reischl, A., von Strachwitz, M.F., Paeth, H., et al., 2020. Tree cooling effects and human thermal comfort under contrasting species and sites. Agric. For. Meteor. 287, 107947.

Regniers, O., 2014. Méthodes d'analyse de texture pour la cartographie d'occupations du sol par télédetection très haute résolution: application à la forêt, la vigne et les parcs ostréicoles. Thesis, Univ. Bordx. 164.

Ren, Z., Zhao, H., Fu, Y., Xiao, L., Dong, Y., 2022. Effects of urban street trees on human thermal comfort and physiological indices: a case study in Changchun city, China. J. For. Res. 33, 911–922.

Russo, A., Escobedo, F.J., Zerbe, S., 2016. Quantifying the local-scale ecosystem services provided by urban treed streetscapes in Bolzano, Italy. AIMS Environ. Sci. 3, 58–76.

Salbitano F., Borelli S., Conigliaro M., Yujuan C., 2016, "Guidelines on urban and peri-urban forestry". FAO Forestry Paper No. 178, Food and Agriculture Organization of the United Nations, Rome, 2016, pp. 158.

Samson, R., Moretti, M., Amorim, J.U., Branquinho, C., Fares, S., et al., 2019. Towards an integrative approach to evaluate the environmental ecosystem services provided by urban forests. J. For. Res. 30, 1981–1996.

Sarp, G., 2014. Spectral and spatial quality analysis of pan-sharpening algorithms: a case study in Istanbul. Eur. J. Remote Sens. 47, 19–28.

Selmi, W., Weber, C., Rivière, E., Blond, N., Mehdi, L., Nowak, D.J., 2016. Air pollution removal by trees in public green spaces in Strasbourg city, France. Urban For. Urban Green. 17, 192–201.

Shojanoori, R., Shafri, H.Z.M., 2016. Review on the use of remote sensing for urban forest monitoring. Arboric. Urban 42, 400–417.

Sicard, P., Agathokleous, E., Anenberg, S.C., De Marco, A., Paoletti, E., Calatayud, V., 2023. Trends in urban air pollution over the last two decades: a global perspective. Sci. Total Environ. 858, 160064.

Sicard, P., Agathokleous, E., Araminiene, V., Carrari, E., Hoshika, Y., De Marco, A., et al., 2018. Should we see urban trees as effective solutions to reduce increasing ozone levels in cities? Environ. Pollut. 243, 163–176.

Sicard, P., Dalstein-Richier, L., 2015. Health and vitality assessment of two common pine species in the context of climate change in Southern Europe. Environ. Res. 137, 235–245.

Silli, V., Salvatori, E., Manes, F., 2015. Removal of airborne particulate matter by vegetation in an urban park in the city of Rome (Italy): an ecosystem services perspective. Ann. di Bot. 5, 53–62.

Singh, K.K., Chen, G., McCarter, J.B., Meentemeyer, R.K., 2015. Effects of LiDAR point density and landscape context on estimates of urban forest biomass. ISPRS J. Photogramm. 101, 310–322.

Smith, R.M., Thompson, K., Hodgson, G.J., Warren, P.H., Gaston, K.J., 2006. Urban domestic gardens: composition and richness of the vascular plant flora, and implications for native biodiversity. Biol. Conserv. 129, 312–322.

Solano, F., Di Fazio, S., Modica, G., 2019. A methodology based on GEOBIA and WorldView-3 imagery to derive vegetation indices at tree crown detail in Olive Orchards. Int. J. Appl. Earth Obs. Geoinf. 83, 101912.

Song, Y., Imanishi, J., Sasaki, T., Ioki, K., Morimoto, Y., 2016. Estimation of broad-leaved canopy growth in the urban forested area using multi-temporal airborne LiDAR datasets. Urban For. Urban Green 16, 142–149.

Southerland V.A., Brauer M., Mohegh A., Hammer M.S., van Donkelaar A., et al., 2022, "Global urban temporal trends in fine particulate matter (PM2.5) and attributable health burdens: estimates from global datasets". Lancet Planet Health 6: e139–46.

Tigges, J., Lakes, T., Hostert, P., 2013. Urban vegetation classification: benefits of multitemporal RapidEye satellite data. Remote Sens. Environ. 136, 66–75.

Ugolini, F., Massetti, L., Calaza-Martínez, P., Cariñanos, P., Dobbs, C., et al., 2020. Effects of the COVID-19 pandemic on the use and perceptions of urban green space: an international exploratory study. Urban For Urban Green 56, 126888.

United Nations, 2020, "The World's Cities in 2016″, Department of Economic and Social Affairs, ISBN 978–92-1–151549-7, available on https://www.un.org.

Vila-Ruiz, C.P., Meléndez-Ackerman, E., Santiago-Bartolomei, R., Garcia-Montiel, D., Lastra, L., et al., 2014. Plant species richness and abundance in residential yards across a tropical watershed: implications for urban sustainability. Ecol. Soc. 19, 22.

Westfall, J., 2015. Spatial-scale considerations for a large-area forest inventory regression model. Forestry 88, 267–274.

Zhang, H., Jim, C.Y., 2014. Species diversity and performance assessment of trees in domestic gardens. Landsc. Urban Plan. 128, 23–34.

Zhang, C., Qiu, F., 2012. Mapping individual tree species in an urban forest using airborne lidar data and hyperspectral imagery. Photogramm. Eng. Remote Sens. 78, 1079–1087.

Zhou, J., Guo, R., Sun, M., Di, T., Wang, S., et al., 2017. The effects of GLCM parameters on LAI estimation using texture values from Quickbird satellite Imagery. Sci. Rep. 7, 7366.

Zhou, W., 2013. An object-based approach for urban land cover classification: Integrating LiDAR height and intensity data. IEEE Geosci. Remote Sens. Lett. 10, 928–931.